Ultra-light axion dark matter

Lam Hui 許林
Columbia University

Collaboration with Jerry Ostriker, Scott Tremaine, Edward Witten

Light axion dark matter

$\text{mass}\, m \sim 10^{-22\pm1}\,\text{eV}$

Fuzzy dark matter
Hu, Barkana, Gruzinov

- A natural candidate for such a light particle is a pseudo Goldstone boson.

- Concrete realization: an angular field of periodicity $2\pi F$ i.e. an axion-like field with a potential from non-perturbative effects (not QCD axion).

$$\mathcal{L} \sim -\frac{1}{2}(\partial\phi)^2 - \Lambda^4(1 - \cos[\phi/F])$$

$$m \sim \Lambda^2/F$$

(see Andreas's talk)

- Relic abundance:

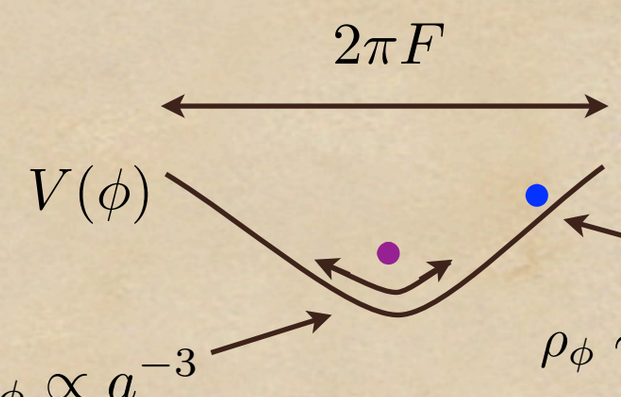

(standard story - see Kolb & Turner; review by Marsh)

$\phi \sim F$ at early times until $H \sim m$

$\rho_\phi \sim m^2F^2$, $\rho_{\text{rad.}} \sim H^2M_{\text{pl}}^2 \sim m^2M_{\text{pl}}^2 \sim T^4$

subsq. oscill. : $\rho_\phi \propto a^{-3}$
self − interaction can be ignored

$$\Omega_{\text{matter}} \sim \left(\frac{F}{10^{17}\,\text{GeV}}\right)^2 \left(\frac{m}{10^{-22}\,\text{eV}}\right)^{1/2}$$

(low scale inflation)

Dynamics of a free massive scalar

- Ignoring self-interaction:

$$-\Box\phi + m^2\phi = 0$$

$m^{-1} \sim 0.06\,\mathrm{pc}$

$(mv)^{-1} \sim 2\ \mathrm{kpc}\ (10\,\mathrm{km\,s^{-1}}/v)$

- Non-relativistic limit:

$$\phi = \frac{1}{\sqrt{2m}}\left[\psi e^{-imt} + \psi^* e^{imt}\right]$$

$$|\ddot{\psi}| \ll m|\dot{\psi}| \longrightarrow i\dot{\psi} = \left[-\frac{\nabla^2}{2m} + m\Phi_{\mathrm{grav.}}\right]\psi$$

- High occupancy implies ψ should be thought of as a classical scalar.
  See simulations by Hsi-Yu Schive, Tzihong Chiueh & Tom Broadhurst, Mocz et al., Veltmaat & Niemeyer (see Jens' talk).
- An alternative viewpoint: ψ as a (classical) fluid.

$$\rho = m\,|\psi|^2 \quad \text{i.e.} \quad \psi = \sqrt{\rho/m}\,e^{i\theta}$$

Recall conservation of probability: current $\propto i(\psi\nabla\psi^* - \psi^*\nabla\psi)$

Reinterpreted as conservation of mass:

$$\dot{\rho} + \nabla\cdot\rho v = 0 \quad \text{where} \quad v = \frac{1}{m}\nabla\theta \qquad \text{i.e. a superfluid.}$$

Fluid formulation (Madelung)

- Euler equation:

$$\dot{v} + v \cdot \nabla v = -\nabla \Phi_{\text{grav.}} + \frac{1}{2m^2} \nabla \left(\frac{\nabla^2 \sqrt{\rho}}{\sqrt{\rho}} \right)$$

"quantum pressure"

- More precisely, an unusual form of stress:

$$T_{ij} = \rho v_i v_j + \frac{1}{2m^2} \left[\partial_i \sqrt{\rho}\, \partial_j \sqrt{\rho} - \sqrt{\rho}\, \partial_i \partial_j \sqrt{\rho} \right]$$

- Can be implemented in standard hydrodynamics codes (Mocz & Succi).

- For linear perturbations (on cosmological bgd.):

Jeans scale $\sim 0.1\,\text{Mpc}$

Perturbations suppressed on small scales - could help avoid small scale problems of standard CDM (Hu, Barkana, Gruzinov: Fuzzy DM ; Amendola, Barbieri).

Typical focus: density profile (cusp versus core), number of satellite galaxies.

Issue: baryonic effects complicate the interpretation of the data.

The unexpected diversity of dwarf galaxy rotation curves

Kyle A. Oman[1,⋆], Julio F. Navarro[1,2], Azadeh Fattahi[1], Carlos S. Frenk[3], Till Sawala[3], Simon D. M. White[4], Richard Bower[3], Robert A. Crain[5], Michelle Furlong[3], Matthieu Schaller[3], Joop Schaye[6], Tom Theuns[3]

[1] *Department of Physics & Astronomy, University of Victoria, Victoria, BC, V8P 5C2, Canada*
[2] *Senior CIfAR Fellow*
[3] *Institute for Computational Cosmology, Department of Physics, University of Durham, South Road, Durham DH1 3LE, United Kingdom*
[4] *Max-Planck Institute for Astrophysics, Garching, Germany*
[5] *Astrophysics Research Institute, Liverpool John Moores University, IC2, Liverpool Science Park, 146 Brownlow Hill, Liverpool, L3 5RF, United Kingdom*
[6] *Leiden Observatory, Leiden University, PO Box 9513, NL-2300 RA Leiden, the Netherlands*

10 July 2015

ABSTRACT

We examine the circular velocity profiles of galaxies in ΛCDM cosmological hydrodynamical simulations from the EAGLE and LOCAL GROUPS projects and compare them with a compilation of observed rotation curves of galaxies spanning a wide range in mass. The shape of the circular velocity profiles of simulated galaxies varies systematically as a function of galaxy mass, but shows remarkably little variation at fixed maximum circular velocity. This is especially true for low-mass dark matter-dominated systems, reflecting the expected similarity of the underlying cold dark matter haloes. This is at odds with observed dwarf galaxies, which show a large diversity of rotation curve shapes, even at fixed maximum rotation speed. Some dwarfs have rotation curves that agree well with simulations, others do not. The latter are systems where the inferred mass enclosed in the inner regions is much lower than expected for cold dark matter haloes and include many galaxies where previous work claims the presence of a constant density "core". The "cusp vs core" issue is thus better characterized as an "inner mass deficit" problem than as a density slope mismatch. For several galaxies the magnitude of this inner mass deficit is well in excess of that reported in recent simulations where cores result from baryon-induced fluctuations in the gravitational potential. We conclude that one or more of the following statements must be true: (i) the dark matter is more complex than envisaged by any current model; (ii) current simulations fail to reproduce the diversity in the effects of baryons on the inner regions of dwarf galaxies; and/or (iii) the mass profiles of "inner mass deficit" galaxies inferred from kinematic data are incorrect.

Key words: dark matter, galaxies: structure, galaxies: haloes

Possible diagnostics of FDM vs conventional CDM:

- dynamical friction

- evaporation of sub-halos by tunneling

- interference

- tidal streams and gravitational lensing

- Lyman-alpha forest

- direct detection

- detection by pulsar timing array

Fornax galaxy and its globular clusters

ESO/Digitized Sky Survey 2

Dynamical friction issue: Tremaine 1976

Dynamical friction

- Chandrasekhar's classic calculation:

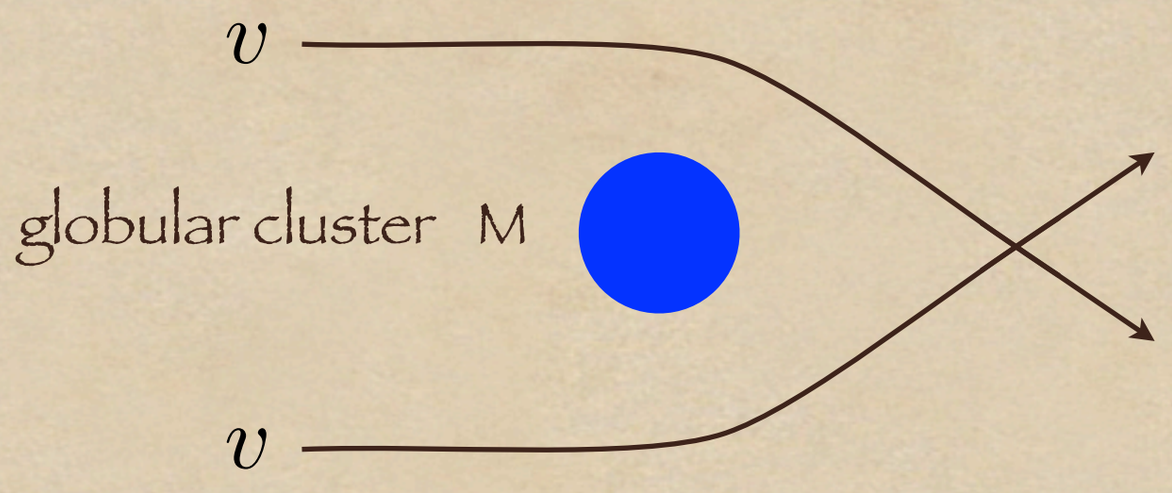

- Quantum stress smooths out density wake, lowering friction.
(see also Lora et al.)

- Use known solution for the Coulomb scattering problem:

$\psi \propto F\left[i\beta, 1, ikr(1 - \cos\theta)\right]$ where F is the confluent hypergeometric func.

$\beta \equiv (GM/v^2)/k^{-1}$ with $k^{-1} = (mv)^{-1}$ = de Broglie wavelength

Small β means quantum stress is important.

- Key - integrate momentum flux to compute friction: $\oint dS_j \; T_{ij}$

Question: shouldn't the quantum and classical answers be identical?

Recall that for Coulomb differential cross section,

quantum = classical.

- But recall also the integrated cross section has a logarithmic divergence.

- Thus, we expect dynamical friction $\propto \ln[r/r_c]$ where $r \sim$ size of galaxy,

$r_c \sim GM/v^2$ or k^{-1}

- This is borne out by analytic calculation, made possible by obscure identities involving hypergeometric functions.

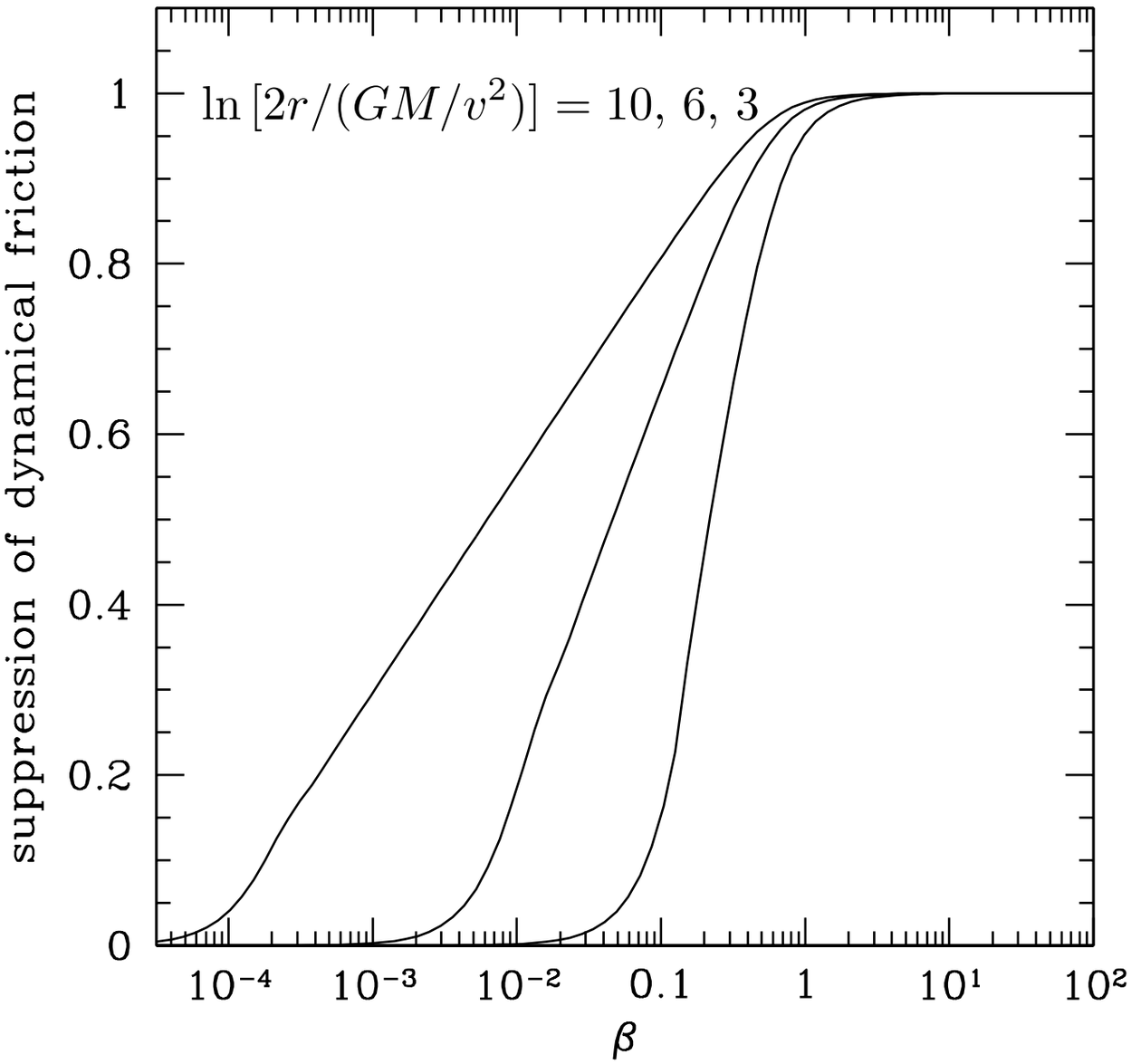

$$\beta \equiv (GM/v^2)/k^{-1}$$
$$= 0.0023 \left(\frac{M}{10^5 M_\odot}\right) \left(\frac{10\,\mathrm{km/s}}{v}\right) \left(\frac{m}{10^{-22}\,\mathrm{eV}}\right)$$

Conclusion:

Given the density profile of a galaxy (which can be experimentally determined), standard CDM has a definite prediction for the dynamical friction, which can be checked against observations.

Fuzzy DM of $m \sim 10^{-22}$ eV can lower dynamical friction by an order of magnitude.

Would be useful to study other systems: Lotz et al. 2001

Possible diagnostics of FDM vs conventional CDM:

- dynamical friction ✓

- evaporation of sub-halos by tunneling

- interference

- tidal streams and gravitational lensing

- Lyman-alpha forest

- direct detection

- detection by pulsar timing array

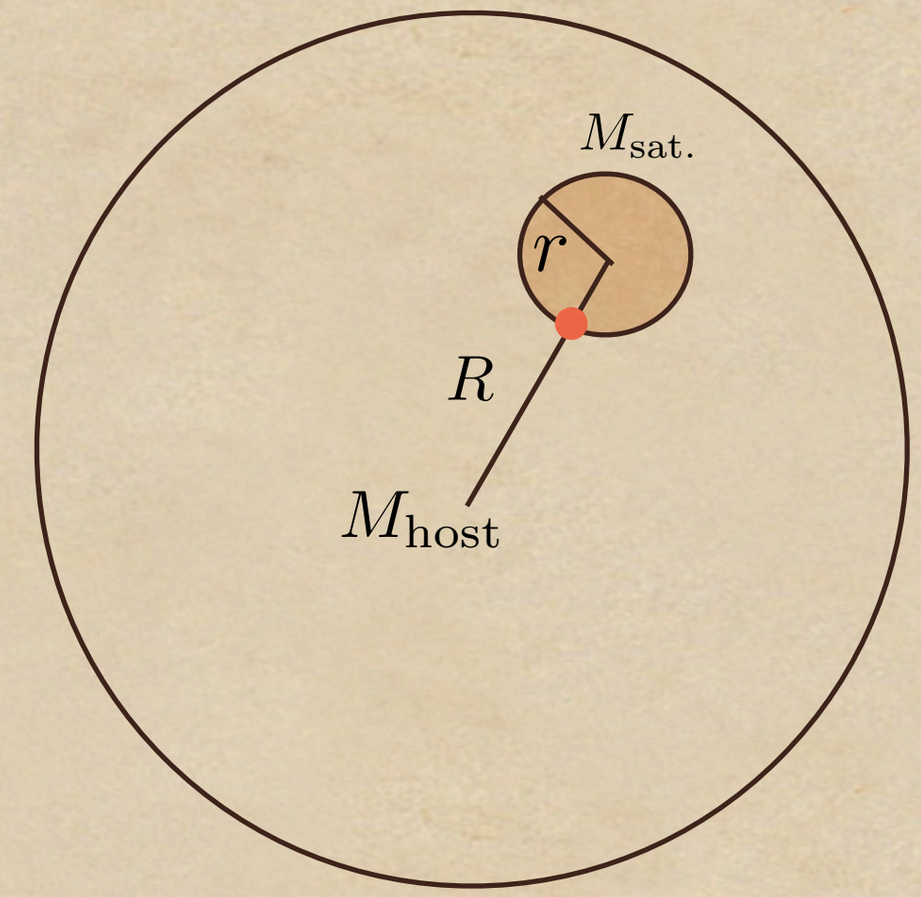

Recall tidal disruption: $$\frac{GM_{\rm host}}{R^2}\frac{r}{R} \sim \frac{GM_{\rm sat.}}{r^2}$$

$r =$ disruption radius

Quantum pressure is expected to alter this.

$M_{\rm satellite} > 10^8 M_\odot$ in Milky Way

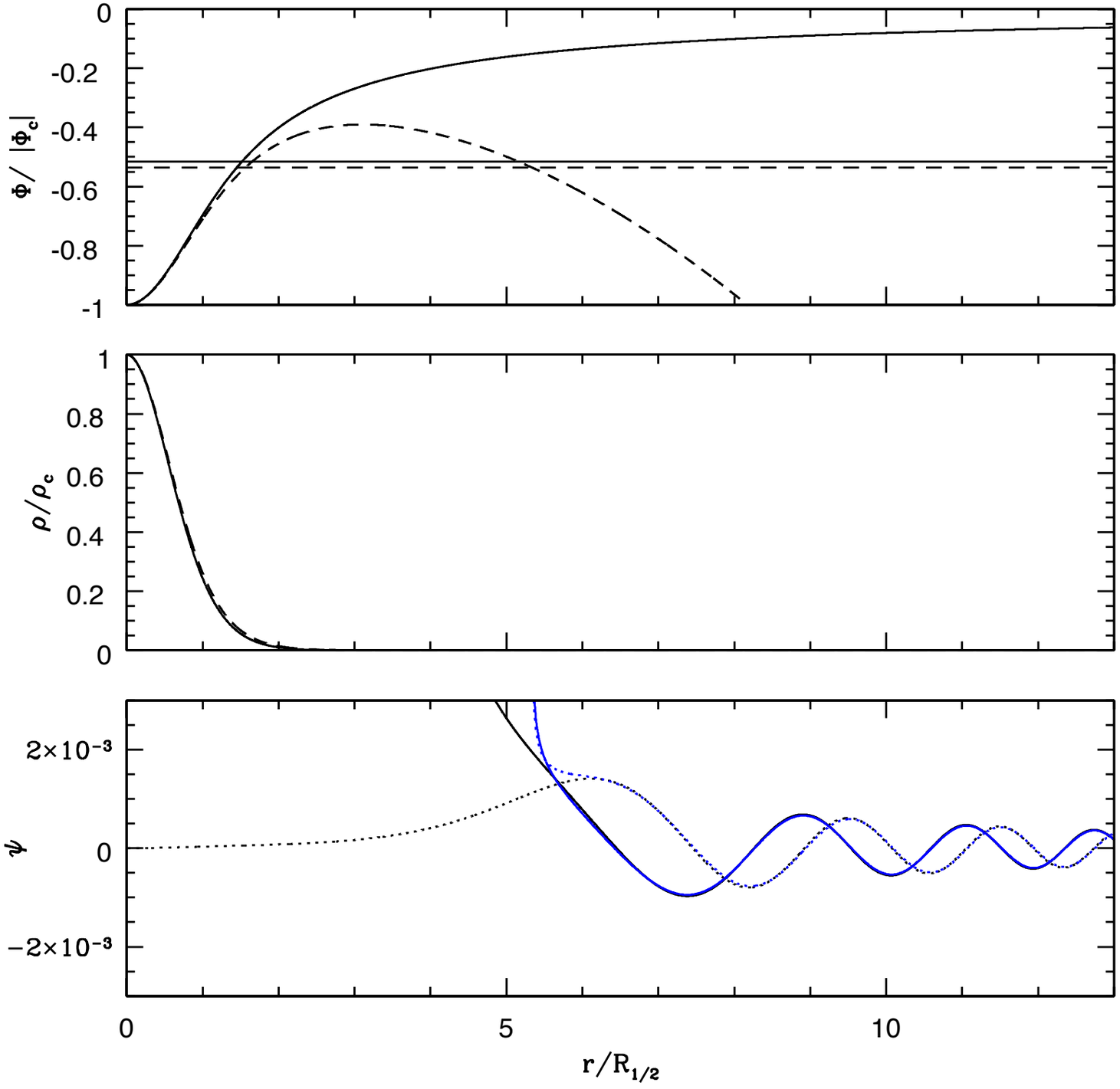

Possible diagnostics of FDM vs conventional CDM:

- dynamical friction ✓

- evaporation of sub-halos by tunneling ✓

- interference

- tidal streams and gravitational lensing

- Lyman-alpha forest

- direct detection

- detection by pulsar timing array

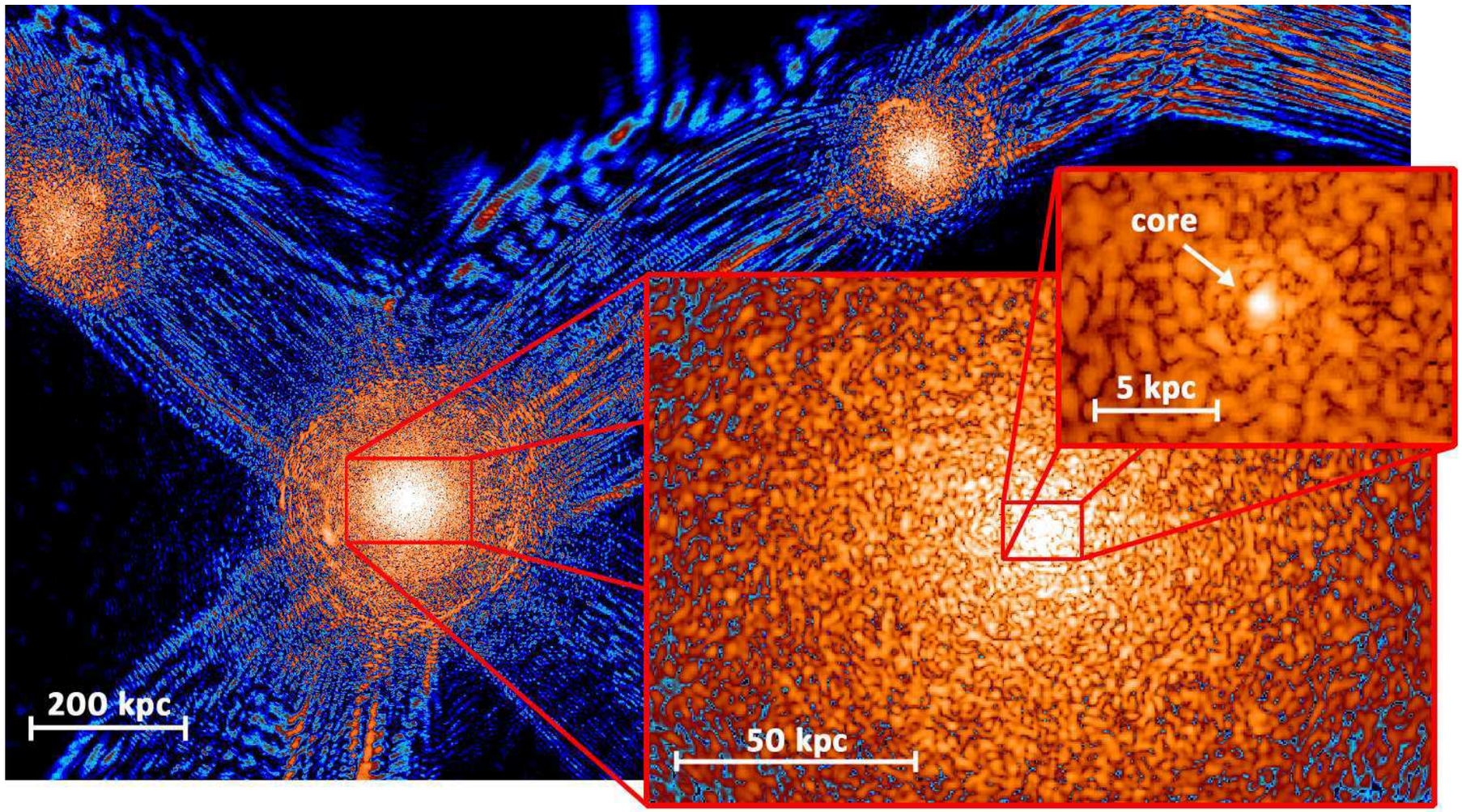

Figure 2: A slice of density field of ψDM simulation on various scales at $z = 0.1$. This scaled sequence (each of thickness 60 pc) shows how quantum interference patterns can be clearly seen everywhere from the large-scale filaments, tangential fringes near the virial boundaries, to the granular structure inside the haloes. Distinct solitonic cores with radius $\sim 0.3 - 1.6$ kpc are found within each collapsed halo. The density shown here spans over nine orders of magnitude, from 10^{-1} to 10^{8} (normalized to the cosmic mean density). The color map scales logarithmically, with cyan corresponding to density $\lesssim 10$.

Schive, Chiueh, Broadhurst

Possible diagnostics of FDM vs conventional CDM:

- dynamical friction ✓

- evaporation of sub-halos by tunneling ✓

- interference ✓

- tidal streams and gravitational lensing

- Lyman-alpha forest

- direct detection

- detection by pulsar timing array

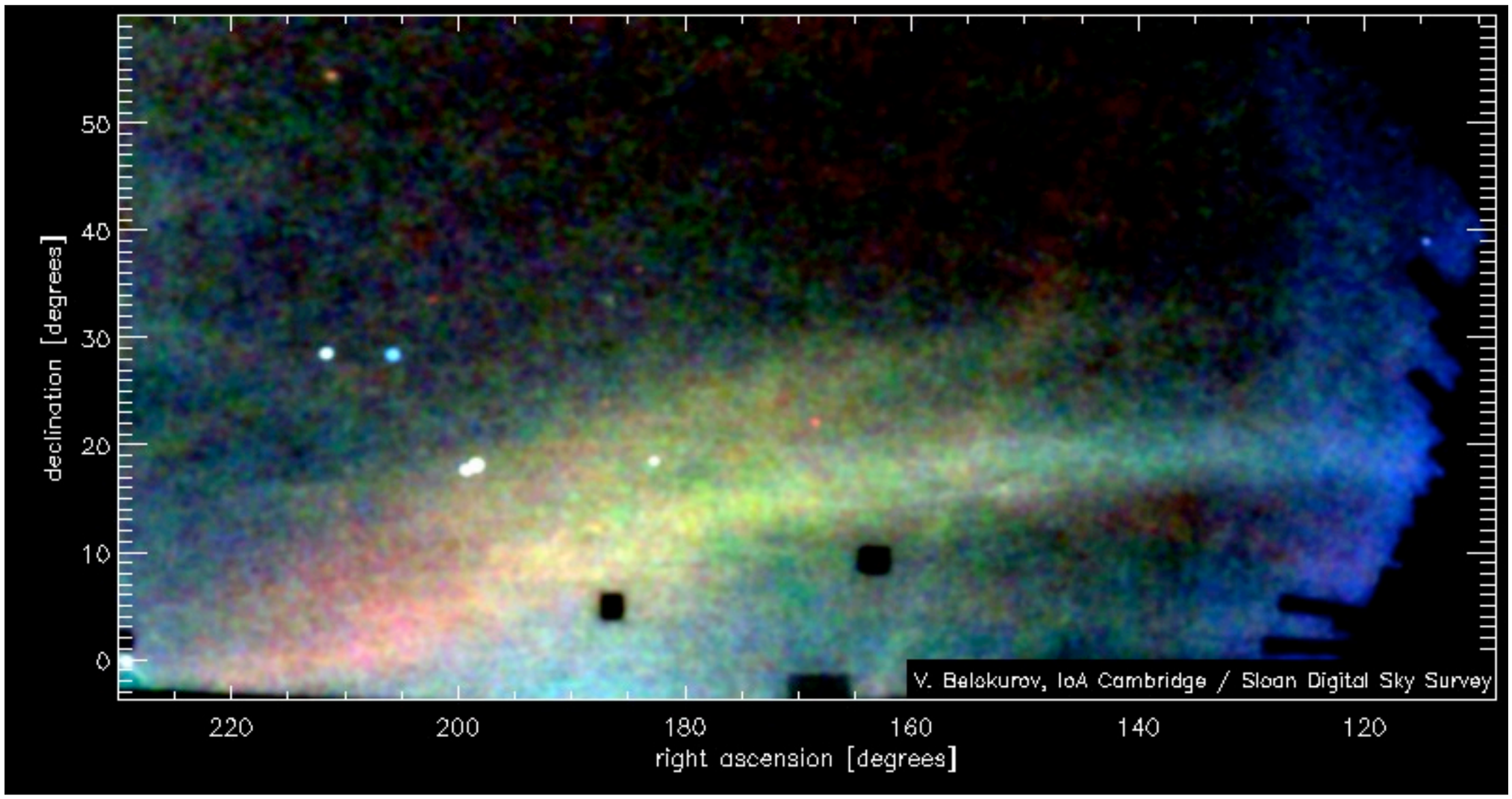

Belokurov, Zucker et al. SDSS II data

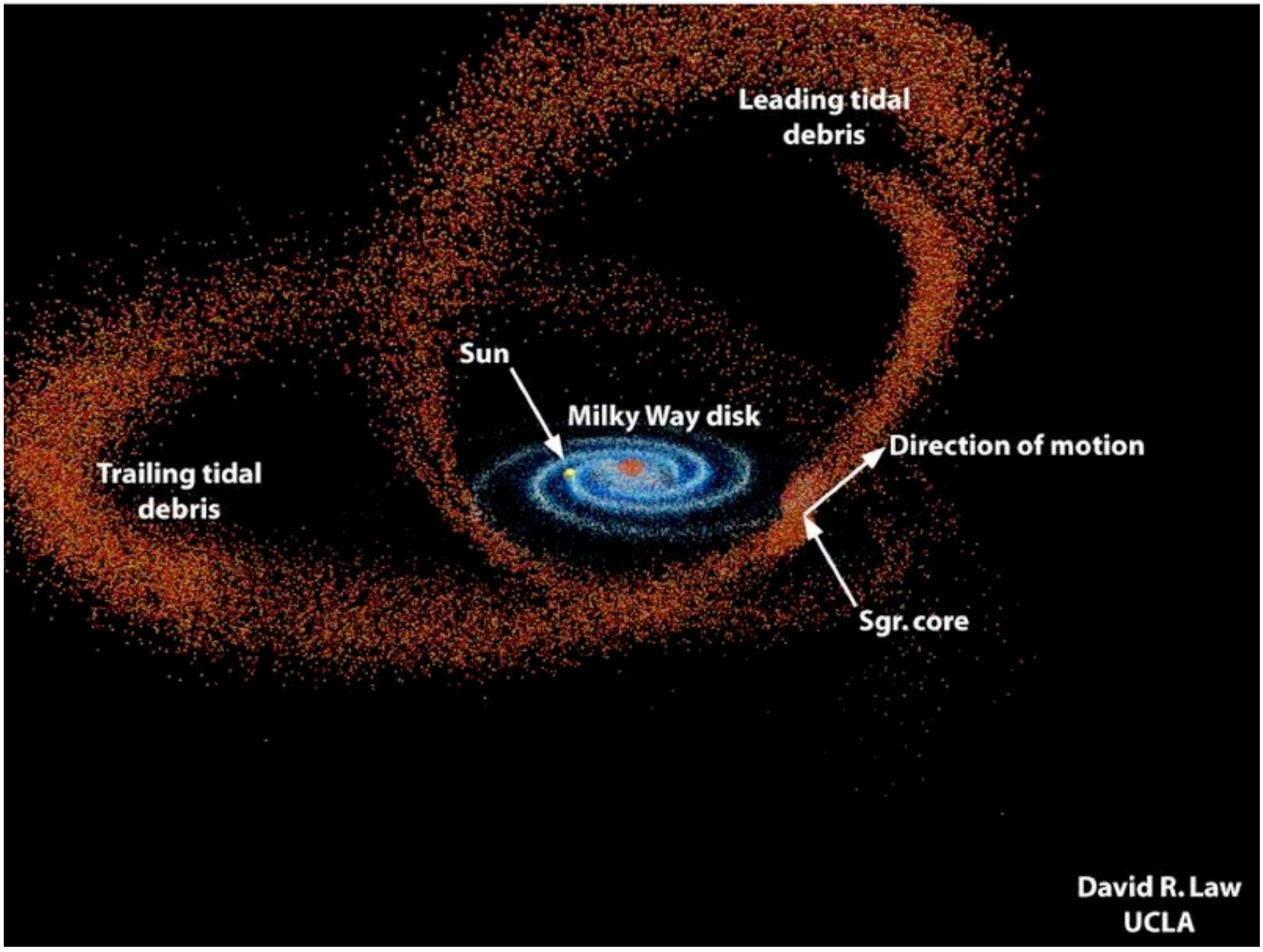

Law, Majewski, Johnston model of Sagittarius stream

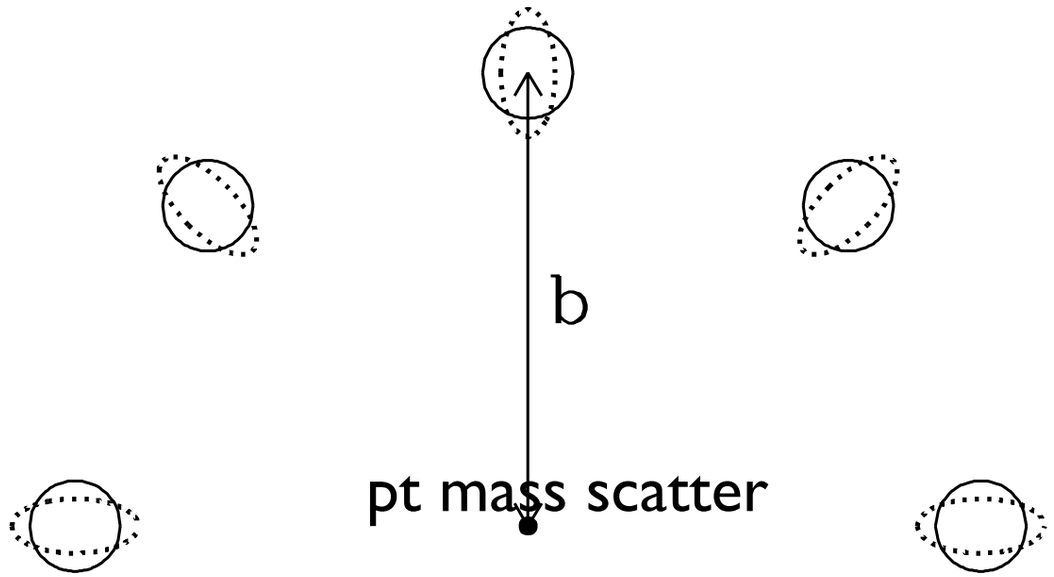
b
pt mass scatter

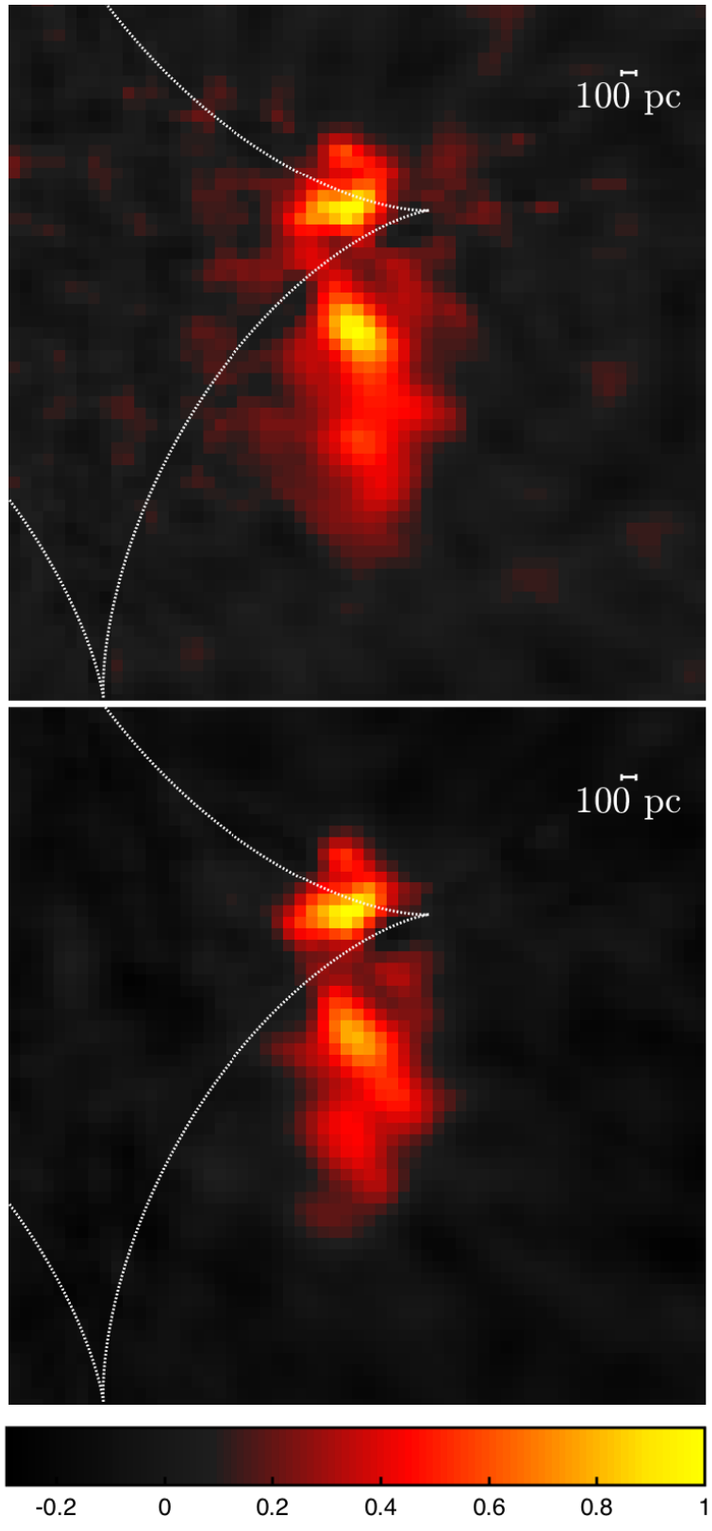

Figure 8. Reconstructed source continuum emission from Band 6 (top panel) and Band 7 (bottom panel) data on a 10 milli-arcsec pixel grid. The white dashed curve shows the tangential caustic predicted by our best-fit smooth model.

Hezaveh, Dalal et al. ALMA

Possible diagnostics of FDM vs conventional CDM:

- dynamical friction ✓

- evaporation of sub-halos by tunneling ✓

- interference ✓

- tidal streams and gravitational lensing ✓

- Lyman-alpha forest

- direct detection

- detection by pulsar timing array

Lyman-alpha forest constraint (WDM) Viel, Becker, Bolton, Haehnelt

(More recent: Irsic et al., Armengaud et al.) [12]

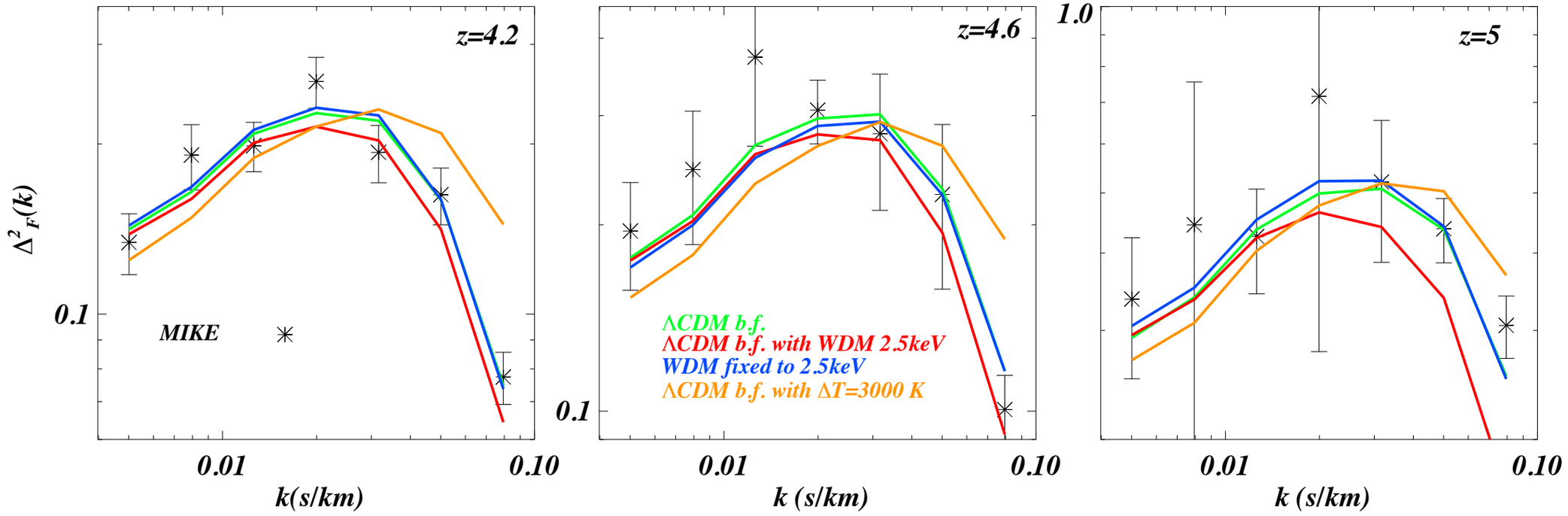

FIG. 11: The best fit model for the MIKE data set (black crosses) used in the present analysis, shown as the green curves and labelled as "ΛCDM b.f.". This model is very close to ΛCDM. We also show for qualitative purposes a few other models: a WDM model that has the same parameters as the best fit model except for the WDM mass (red curves) which is chosen to be 2.5 keV; a model that has a hotter temperature (orange curves) and a model for which the mass of the WDM is fixed to $m_{\rm WDM} = 2.5$ keV, but for which all other parameters are set to their best-fitting values for this choice (blue curves). Note that for the MIKE data we do not use the $z = 5.4$ redshift bin.

Naive translation : $m_{\rm WDM} \sim 2.5\,{\rm keV} \rightarrow m_{\rm FDM} \sim 10^{-21}\,{\rm eV}$

But :
- allowing non – montonic thermal history relaxes WDM mass bound by 1 keV (Garzilli et al.)
- fluctuations in the ionizing background and reionization history could be important
- granularity of FDM might be non – negligible

The impact of feedback from galaxy formation on the Lyman-α transmitted flux

Matteo Viel[1,2], Joop Schaye[3] & C. M. Booth[3,4,5]
[1] *INAF - Osservatorio Astronomico di Trieste, Via G.B. Tiepolo 11, I-34131 Trieste, Italy (viel@oats.inaf.it)*
[2] *INFN/National Institute for Nuclear Physics, Via Valerio 2, I-34127 Trieste, Italy*
[3] *Leiden Observatory, Leiden University, P.O. Box 9513, 2300 RA Leiden, the Netherlands*
[4] *Department of Astronomy and Astrophysics, The University of Chicago, Chicago, IL 60637, USA*
[5] *Kavli Institute for Cosmological Physics and Enrico Fermi Institute, The University of Chicago, Chicago, IL 60637, USA*

28 November 2012

ABSTRACT
The forest of Lyman-α absorption lines seen in the spectra of distant quasars has become an important probe of the distribution of matter in the Universe. We use large, hydrodynamical simulations from the OWLS project to investigate the effect of feedback from galaxy formation on the probability distribution function and the power spectrum of the Lyman-α transmitted flux. While metal-line cooling is unimportant, both galactic outflows from massive galaxies driven by active galactic nuclei and winds from low-mass galaxies driven by supernovae have a substantial impact on the flux statistics. At redshift $z = 2.25$, the effects on the flux statistics are of a similar magnitude as the statistical uncertainties of published data sets. The changes in the flux statistics are not due to differences in the temperature-density relation of the photo-ionised gas. Instead, they are caused by changes in the density distribution and in the fraction of hot, collisionally ionised gas. It may be possible to disentangle astrophysical and cosmological effects by taking advantage of the fact that they induce different redshift dependencies. In particular, the magnitude of the feedback effects appears to decrease rapidly with increasing redshift. Analyses of Lyman-α forest data from surveys that are currently in process, such as BOSS/SDSS-III and X-Shooter/VLT, must take galactic winds into account.

Key words: cosmology: theory – methods: numerical – galaxies: intergalactic medium - quasars: absorption lines

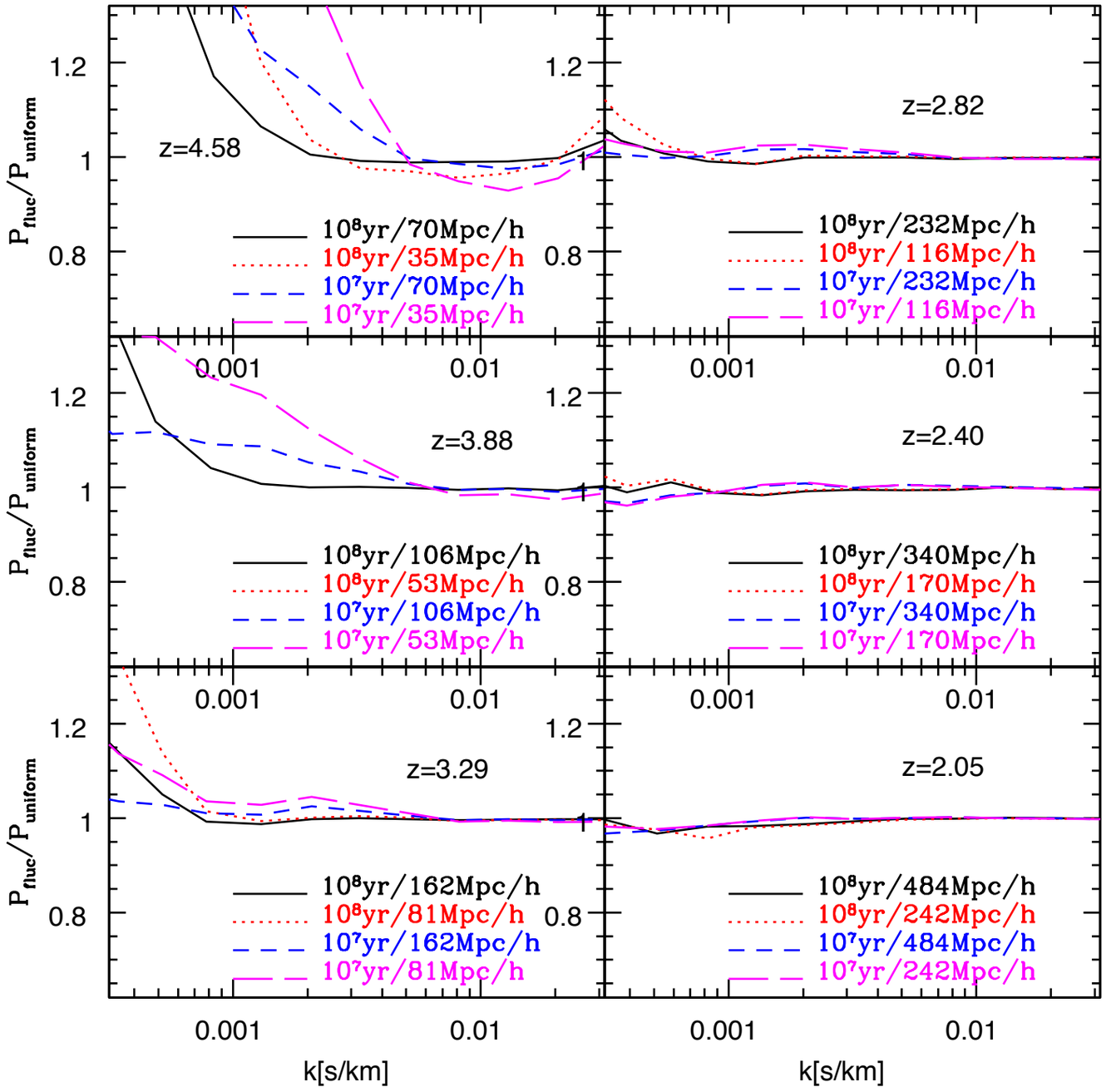

Figure 6. Same as figure 5 using bright end slope of the quasar luminosity function $\beta = 2.58$.

McDonald et al. 2004

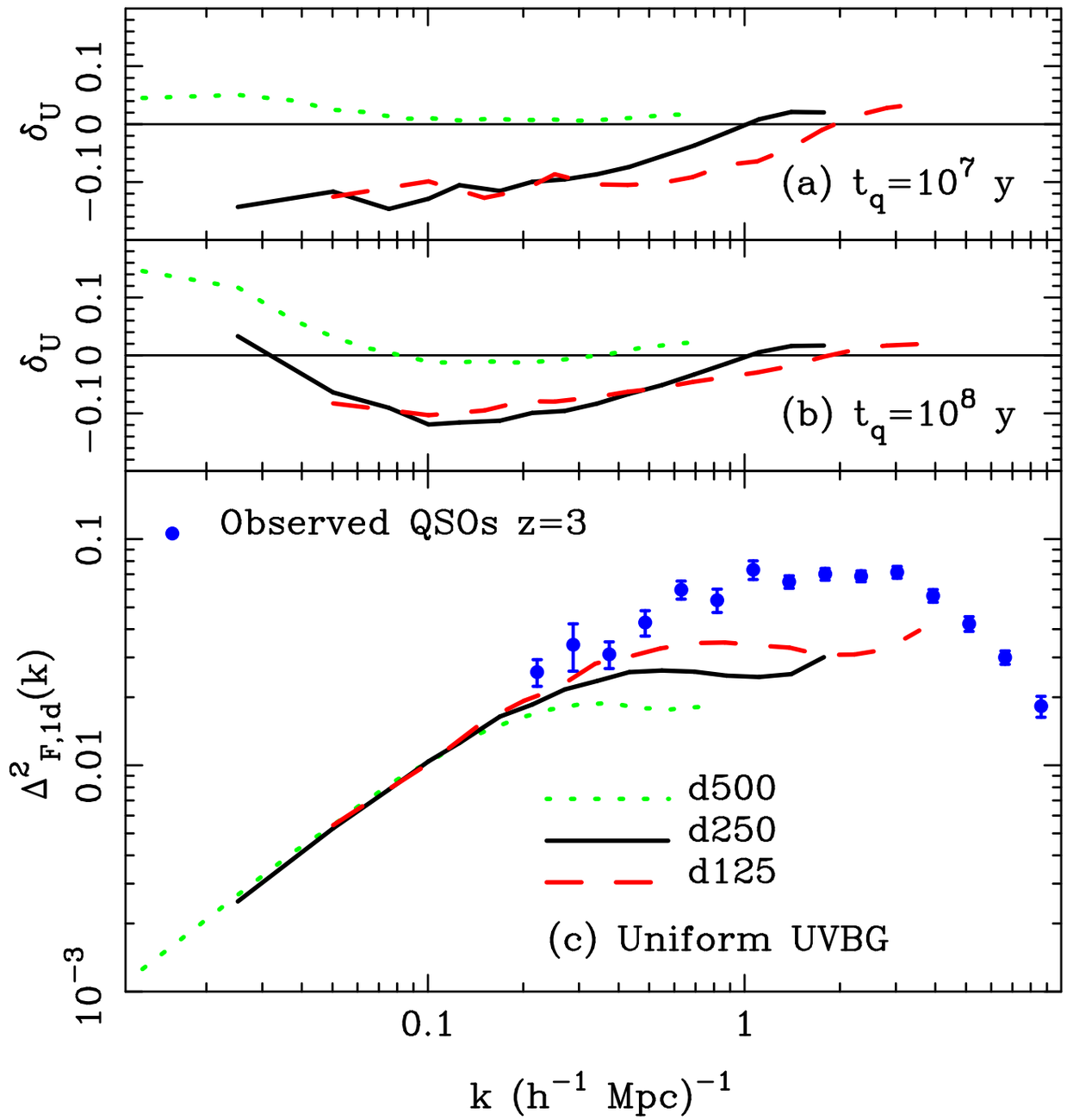

FIG. 9.— Convergence test for the box size, force resolution an particle mass. We show the power spectrum of the Lyα forest flu $\Delta^2_{\rm F}(k)$ averaged over all realizations for the three sets of simulatior with different box sizes and particle masses. In this case output wa on the lightcone, but the radiation output of quasars was set to b isotropic. The top panel shows the fractional difference (Eqn. 16) i $\Delta^2_{\rm F}(k)$ between the raytraced simulation and that using a uniforı radiation field.

Croft 2003

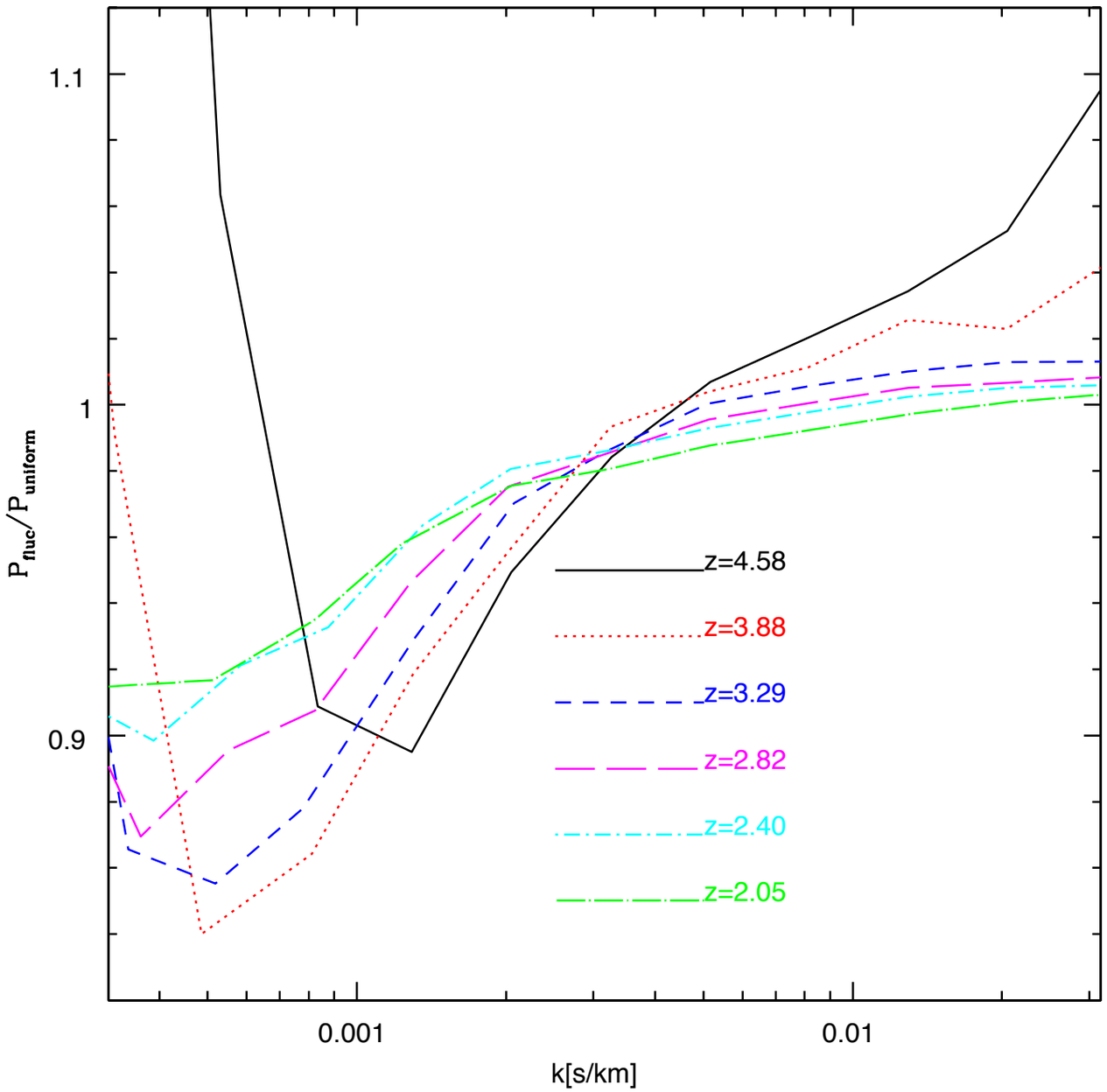

Figure 7. Example of the effect on the flux power spectrum if the sources of ionizing radiation are galaxies with density comparable to that of LBGs. We find a suppression of power in this case.

McDonald et al. 2004

Spread of temperature (at mean density) increases as z → reionization.

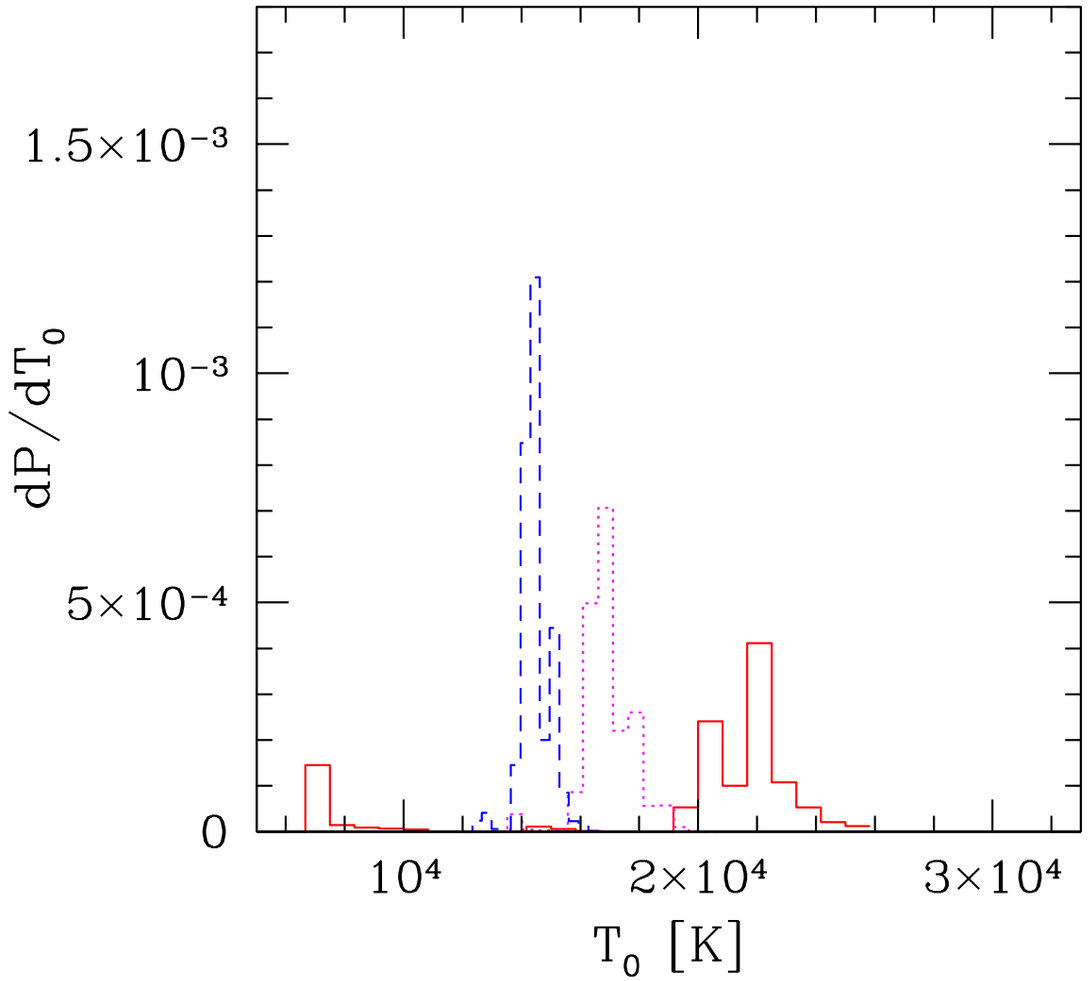

LH, Haiman

Possible diagnostics of FDM vs conventional CDM:

- dynamical friction ✓

- evaporation of sub-halos by tunneling ✓

- interference ✓

- tidal streams and gravitational lensing ✓

- Lyman-alpha forest ✓

- direct detection

- detection by pulsar timing array

from Kim, Marsh 2015 (see also Graham, Rajendran 2013, Budker et al. 2013)

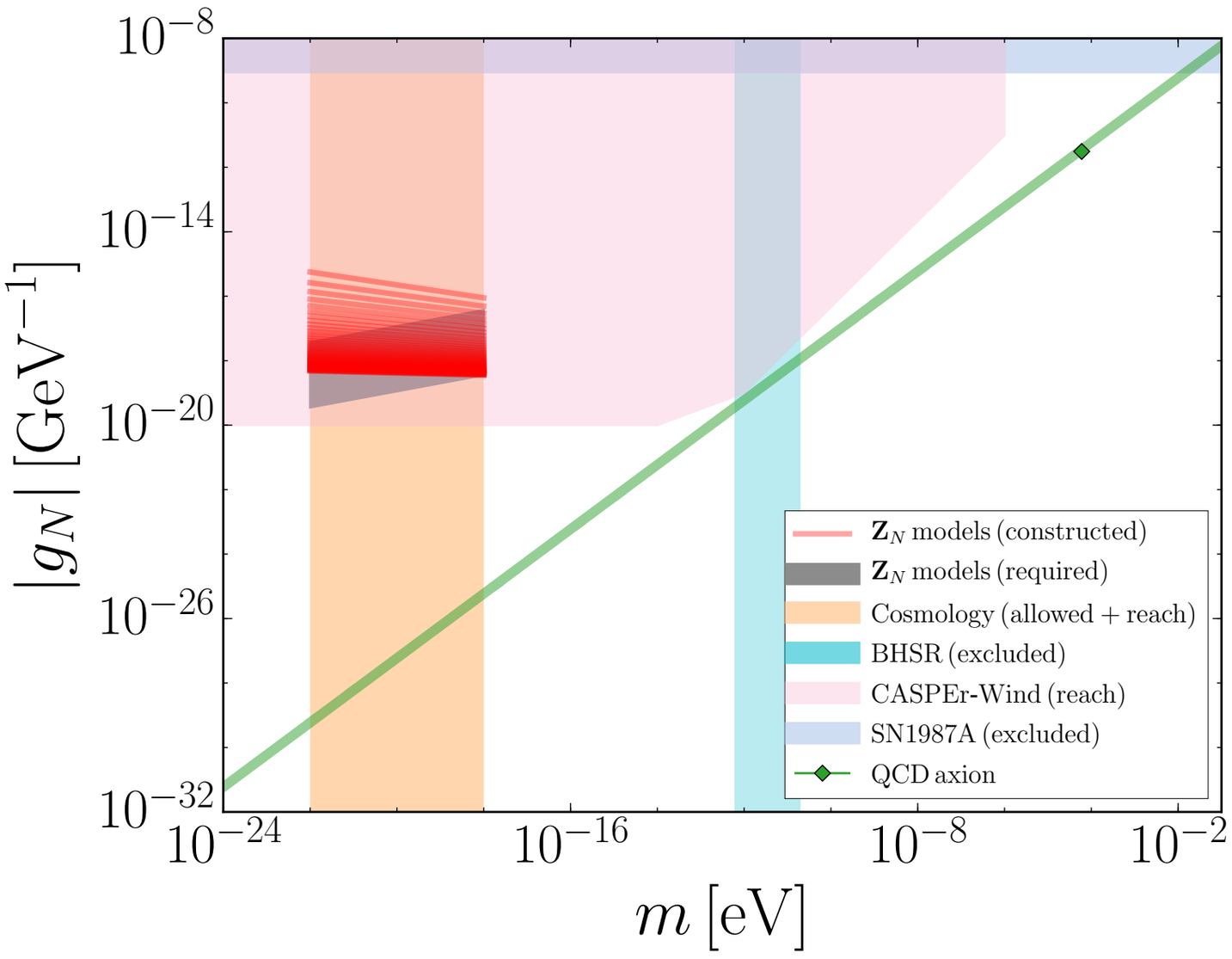

$$\partial_\mu \phi \, \bar{\Psi} \gamma^\mu \gamma_5 \Psi$$

FIG. 3: Axion parameter space, (m, g_N). The QCD axion paired with the ULA is shown for reference, along with the specific point $f_{\rm QCD} = 10^{11}$ GeV, which is our reference value. BHSR excludes a range of masses at 2σ independent of DM abundance and coupling strength [76]. SN1987A excludes the shaded region with $g_N \gtrsim 8.2 \times 10^{-10}$, independent of DM abundance and axion mass [79]. The region both allowed and detectable using cosmology, and relevant to the small-scale crises of CDM is 10^{-22} eV $\lesssim m \lesssim 10^{-18}$ eV [24–26, 28–30]. We show the $\mathbf{Z}_N$ models in this regime only, and also show the target region where $f_{\rm ULA}$ allows for the ULAs to be the dominant form of DM without fine tuning. The region accessible to direct detection using the spin precession technique of CASPEr-Wind [34, 35] is also shown. The cosmologically relevant regime of the $\mathbf{Z}_N$ models lies well within the projected sensitivity of CASPEr-Wind, and is not excluded by any other probes.

Search for axion-like dark matter through nuclear spin precession in electric and magnetic fields

C. Abel,[1] N. J. Ayres,[1,*] G. Ban,[2] G. Bison,[2] K. Bodek,[3] V. Bondar,[4] M. Daum,[2] M. Fairbairn,[5] V. V. Flambaum,[6,7] P. Geltenbort,[8] K. Green,[9] W. C. Griffith,[1] M. van der Grinten,[9] Z. D. Grujić,[10] P. G. Harris,[1] N. Hild,[2] P. Iaydjiev,[9,11] S. N. Ivanov,[9,12] M. Kasprzak,[4] Y. Kermaidic,[13] K. Kirch,[14,2] H.-C. Koch,[2] S. Komposch,[2,14] P. A. Koss,[4] A. Kozela,[15] J. Krempel,[14] B. Lauss,[2] T. Lefort,[16] Y. Lemière,[16] D. J. E. Marsh,[5] P. Mohanmurthy,[2,14] A. Mtchedlishvili,[2] M. Musgrave,[17] F. M. Piegsa,[18] G. Pignol,[13] M. Rawlik,[14,†] D. Rebreyend,[13] D. Ries,[18,2,14] S. Roccia,[19] D. Rozpędzik,[3] P. Schmidt-Wellenburg,[2] N. Severijns,[4] D. Shiers,[1] Y. V. Stadnik,[6,7] A. Weis,[10] E. Wursten,[4] J. Zejma,[3] and G. Zsigmond[2]

[1] *Department of Physics and Astronomy, University of Sussex, Falmer, Brighton BN1 9QH, United Kingdom*
[2] *Paul Scherrer Institute, CH-5232 Villigen PSI, Switzerland*
[3] *Institute of Physics, Jagiellonian University in Krakow, Poland*
[4] *Instituut voor Kern en Stralingsfysica, Katholieke Universiteit Leuven, B-3001 Leuven, Belgium*
[5] *King's College London Department of Physics, London, WC2R 2LS, United Kingdom*
[6] *School of Physics, University of New South Wales, Sydney 2052, Australia*
[7] *Johannes Gutenberg University, 55122 Mainz, Germany*
[8] *Institut Laue-Langevin, BP 156, F-38042 Grenoble Cedex 9, France*
[9] *Rutherford Appleton Laboratory, Chilton, Didcot, Oxon OX11 0QX, UK*
[10] *Physics Department, University of Fribourg, Fribourg, Switzerland*
[11] *Present address: Institute of Nuclear Research and Nuclear Energy, Sofia, Bulgaria*
[12] *Present address: Petersburg Nuclear Physics Institute, Russia*
[13] *LPSC, Université Grenoble Alpes, CNRS/IN2P3, Grenoble, France*
[14] *ETH Zürich, Institute for Particle Physics, CH-8093 Zürich, Switzerland*
[15] *Institute of Nuclear Physics, Polish Academy of Sciences, Krakow, Poland*
[16] *Normandie Univ, ENSICAEN, UNICAEN, CNRS/IN2P3, LPC Caen, 14000 Caen, France*
[17] *Laboratory for Nuclear Science, Massachusetts Institute of Technology, Cambridge, MA 02139, USA*
[18] *Laboratory for High Energy Physics, University of Bern, CH-3012 Bern, Switzerland*
[19] *CSNSM, Université Paris Sud, CNRS/IN2P3, Orsay campus, France*

(Dated: August 23, 2017)

We report on a search for ultra-low-mass axion-like dark matter by analysing the ratio of the spin-precession frequencies of stored ultracold neutrons and ^{199}Hg atoms for an axion-induced oscillating electric dipole moment of the neutron and an axion-wind spin-precession effect. No signal consistent with dark matter is observed for the axion mass range 10^{-24} eV $\leq m_a \leq 10^{-17}$ eV. Our null result sets the first laboratory constraints on the coupling of axion dark matter to gluons, which improve on astrophysical limits by up to 3 orders of magnitude, and also improves on previous laboratory constraints on the axion coupling to nucleons by up to a factor of 40.

Possible diagnostics of FDM vs conventional CDM:

- dynamical friction ✓

- evaporation of sub-halos by tunneling ✓

- interference ✓

- tidal streams and gravitational lensing ✓

- Lyman-alpha forest ✓

- direct detection ✓

- detection by pulsar timing array

Pulsar timing signal from ultralight scalar dark matter

Andrei Khmelnitsky[a] **and Valery Rubakov**[b,c]

[a] *Arnold Sommerfeld Center for Theoretical Physics,*
Ludwig Maximilians University,
Theresienstr. 37, 80333 Munich, Germany

[b] *Institute for Nuclear Research of the Russian Academy of Sciences,*
60th October Anniversary Prospect, 7a, 117312 Moscow, Russia

[c] *Department of Particle Physics and Cosmology, Physics Faculty,*
M.V. Lomonosov Moscow State University,
Vorobjevy Gory, 119991, Moscow, Russia

Abstract: An ultralight free scalar field with mass around $10^{-23} - 10^{-22}$ eV is a viable dark mater candidate, which can help to resolve some of the issues of the cold dark matter on sub-galactic scales. We consider the gravitational field of the galactic halo composed out of such dark matter. The scalar field has oscillating in time pressure, which induces oscillations of gravitational potential with amplitude of the order of 10^{-15} and frequency in the nanohertz range. This frequency is in the range of pulsar timing array observations. We estimate the magnitude of the pulse arrival time residuals induced by the oscillating gravitational potential. We find that for a range of dark matter masses, the scalar field dark matter signal is comparable to the stochastic gravitational wave signal and can be detected by the planned SKA pulsar timing array experiment.

See also Martino, Broadhurst, Tye, Chiueh, Schive, Lazkoz
Blas, Nacir, Sibiryakov

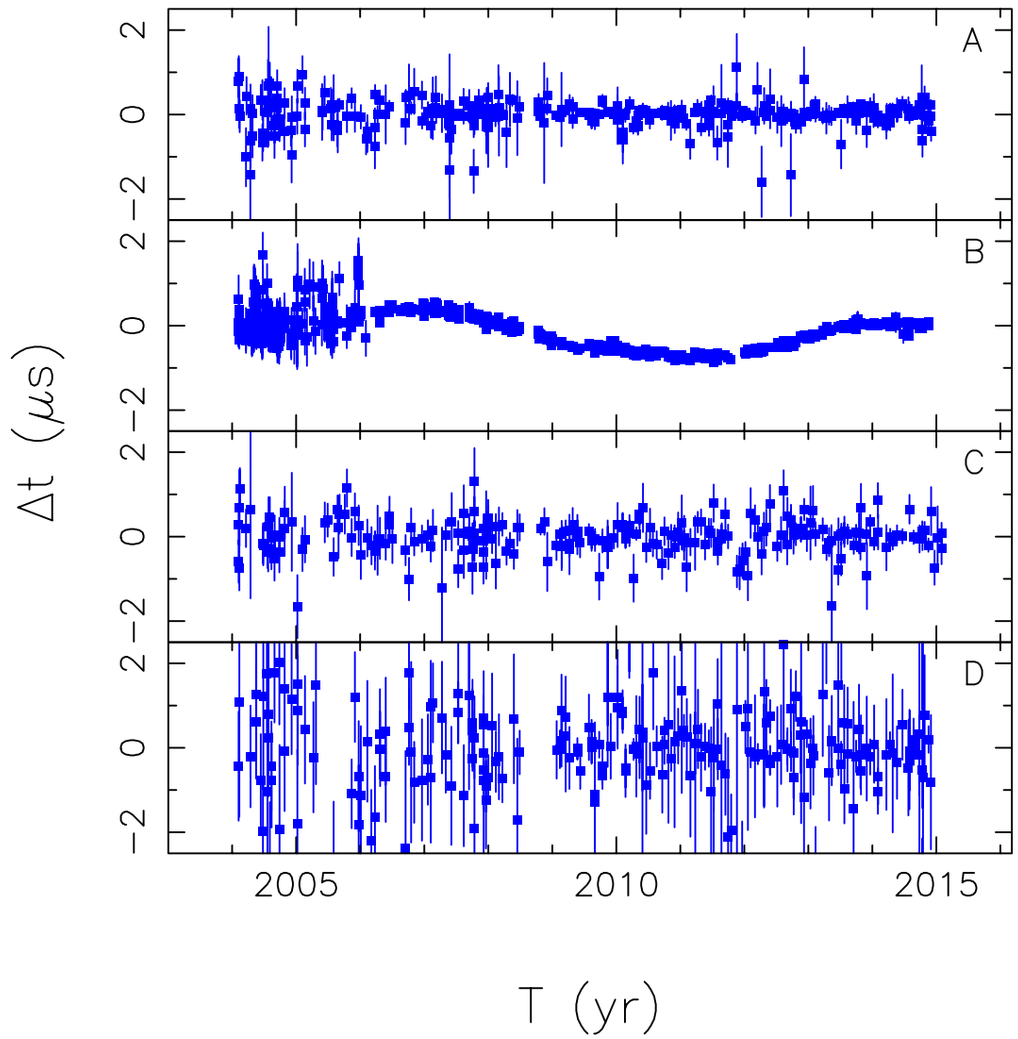

Fig. 1. **Residual pulse times of arrival, Δ*t*, for the four pulsars used in our analysis**. These are PSR J1909-3744 (panel *A*), PSR J0437-4715 (panel B), PSR J1713+0747 (panel *C*), and PSR J1744-1134 (panel *D*).

Shannon et al.

Possible diagnostics of FDM vs conventional CDM:

- dynamical friction ✓

- evaporation of sub-halos by tunneling ✓

- interference ✓

- tidal streams and gravitational lensing ✓

- Lyman-alpha forest ✓

- direct detection ✓

- detection by pulsar timing array ✓

Additional slides follow.

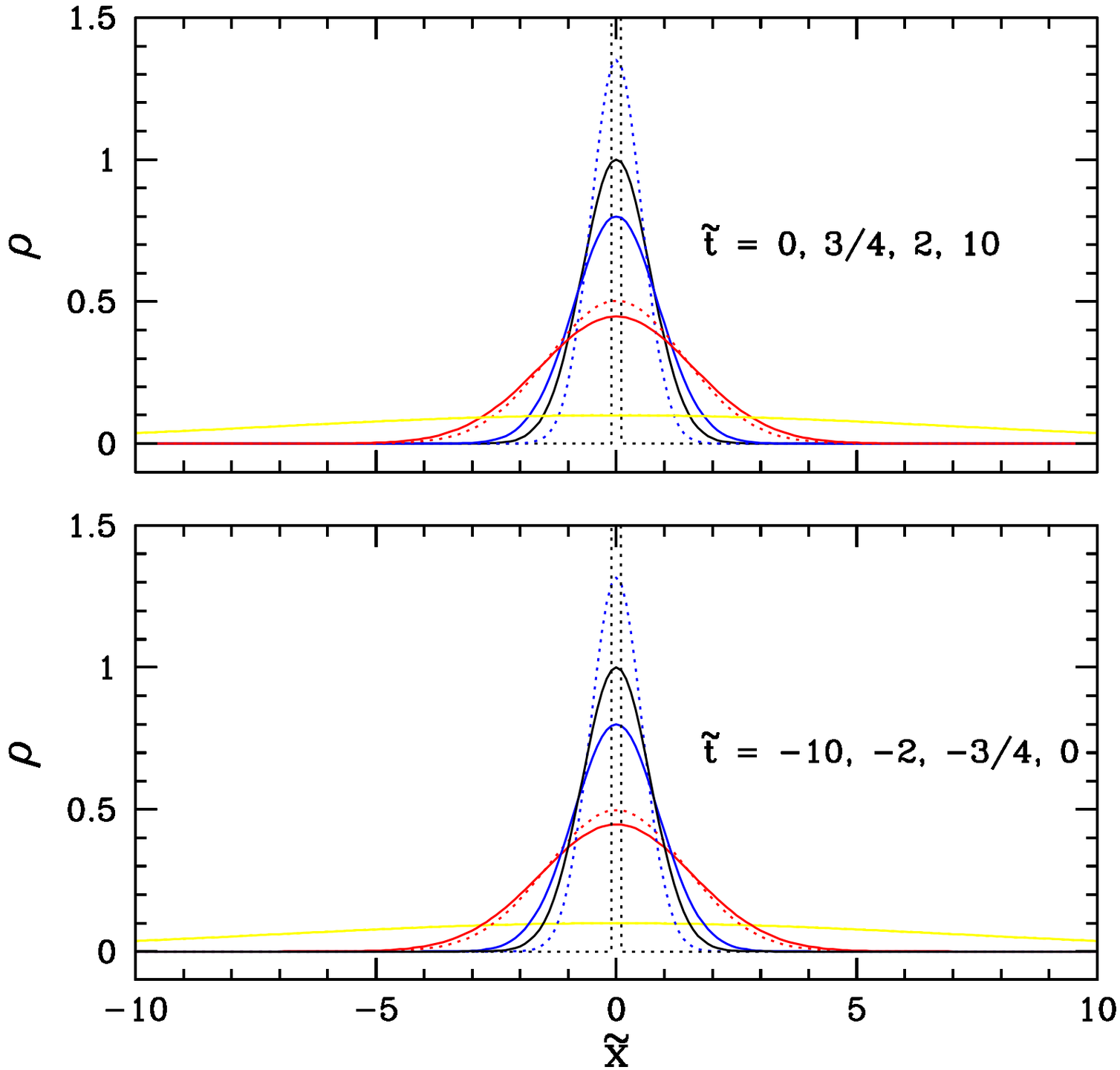
1.5
1
0.5
0
ρ
t̃ = 0, 3/4, 2, 10
1.5
1
0.5
0
ρ
t̃ = −10, −2, −3/4, 0
−10
−5
0
5
10
x̃

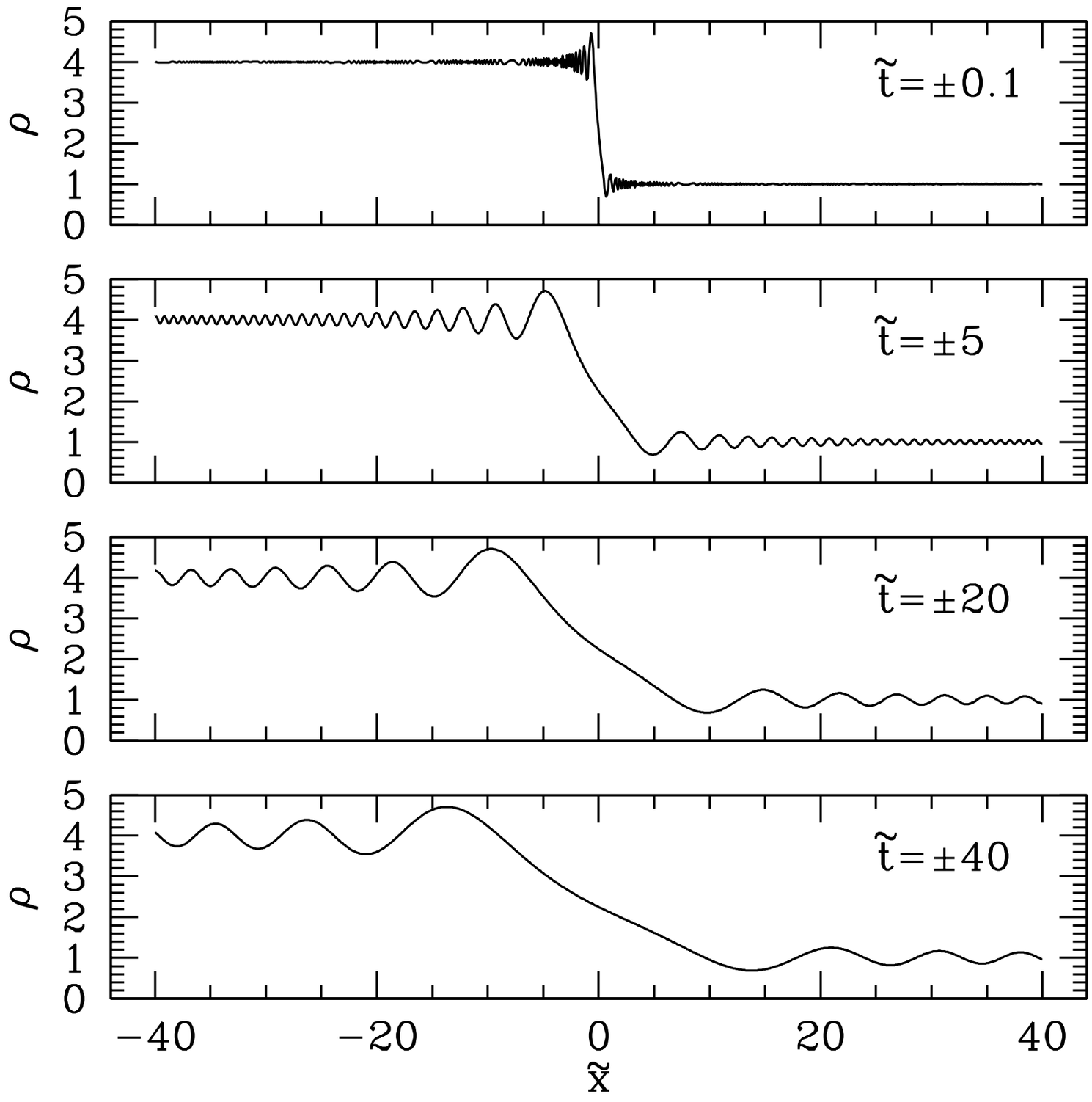
ρ
5
4
3
2
1
0
t̃ = ±0.1
t̃ = ±5
t̃ = ±20
t̃ = ±40
−40
−20
0
20
40
x̃

Average shear vanishes, but rms shear builds up in a random walk.

$$\text{rms shear of tidal stream} \sim N^{3/2} R^{-1} \int d^2 k_\perp P_\delta(k_\perp)$$

where $R =$ orbital radius, $N =$ no. of orbits,

$P_\delta =$ substructure power spectrum

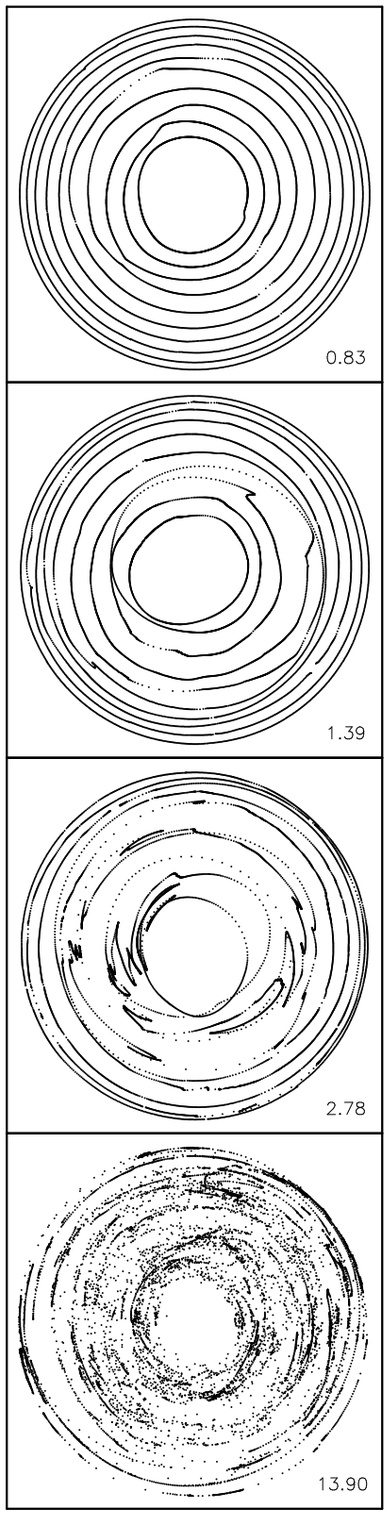

FIG. 1.— Face on views of a time sequence within one simulation. A range of stream locations are sampled with ten rings with 1000 particles per ring. These idealized streams are initiated on purely circular orbits which would preserve their appearance in the absence of sub-halos. The time is shown in Gyr indicated in the lower right of each sub-panel. The plotted radii are the arctangent of the r_{max} scaled radii to allow a more uniform display. Note how a wave-like perturbation evolves into a z-fold which gradually leads to a scrambling of the ring.

Carlberg 2009